Low-Valency Nitridocobaltates of Alkaline-Earth Elements and Related Compounds

Peter Höhn, Joanna K. Bendyna, Alim Ormeci, Walter Schnelle, and Rüdiger Kniep

Introduction

Nitridometalates of the transition elements – a long running research project at our institute [1-3] – reveal a wide spectrum of novel crystal structures. They display interesting physical properties due to the high polarizability of the nitride ion and the low oxidation states of the transition metals. Nitridocobaltates and –nickelates have exclusively low-valence states (Co^{-I}, $Ni^{0,I}$) and linear coordination of Co and Ni by nitrogen. Reports on higher oxidation states of Co and Ni ($Ca_3Co^{III}N_3$ [4] and $Sr_2Ni^{II}N_2$ [5]) were corrected after reinvestigation ([3,6,7] and this work).

Three different motifs of complex nitridocobaltate and –nickelate anions are known up to now from alkaline-earth compounds (Fig. 1): isolated dumbbells $[M^{I}N_2]^{5-}$ (e.g. $Ca_5[Co^{I}N_2]_2$ [8]), 1D infinite chains $^{1}_{\infty}[M^{I}N^{2-}]$ in various conformations (e.g. $Ba_8[Ni^{I}N]_6N$ [9]), and 2D layers $^{2}_{\infty}[M^{0,I}{}_3N_2^{4-}]$ ($Ba_2[Ni^{0,I}{}_3N_2]$ [2, 10]).

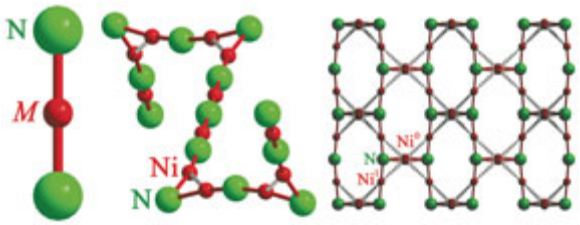

Fig. 1: Structural motifs of complex nitridocobaltate and nitridonickelate anions in alkaline-earth compounds: dumbbells $[M^{I}N_2]^{5-}$ (left), infinite chains $^{1}_{\infty}[M^{I}N^{2-}]$ (center), layers $^{2}_{\infty}[M^{0,I}{}_2N_3{}^{4-}]$ (right).

Preparation

The synthesis of low-valency nitridocobaltates and nitridonickelates is done from appropriate mixtures of the binary alkaline-earth nitrides and the corresponding transition elements at temperatures between 750° C and 1100° C. Due to the air and moisture sensitivity of starting materials and reaction products, all manipulations have to be performed under inert conditions.

Based on our recent interests in carbometalates [11], we also investigated the effect of carbon additives to selected nitridometalate systems.

As already shown [3,6], the formation of cyano-nitrido-metalates such as $Sr_2[NNi(CN)]$ takes place preferably in reducing atmospheres. Nitridometalate-carbodiimides are formed from mixtures of alkaline-earth metals, transition elements, and carbon at temperatures between 700 °C and 1150 °C under oxidizing (nitrogen-rich) conditions.

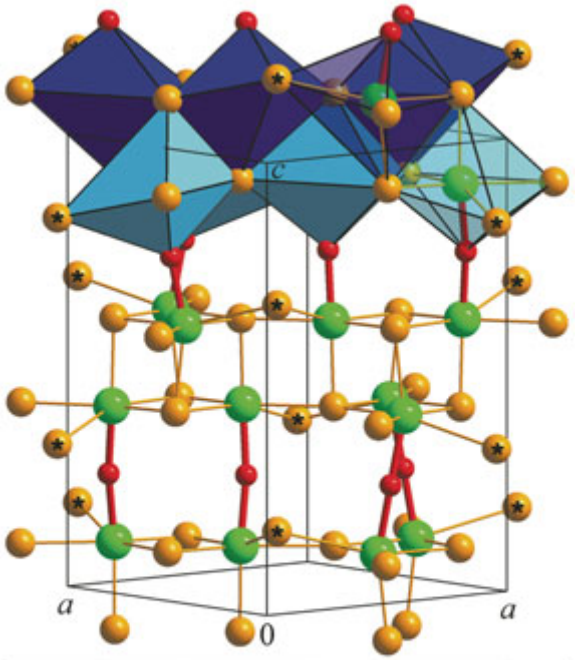

$AE_5[Co^{I}N_2]_2$	a [Å]	c [Å]	V [Å^3]
$Ca_5[CoN_2]_2$	8.0767(1)	12.1401(2)	791.94(2)
$Sr_5[CoN_2]_2$	8.326(2)	12.242(4)	848.7(4)
$BaCa_4[CoN_2]_2$	8.3422(3)	12.2201(8)	850.42(7)

Fig. 2: Crystal structure of $AE_5[Co^{I}N_2]_2$. Dumbbells $[Co^{I}N_2]^{5-}$ in nearly parallel arrangement forming layers parallel (001) interconnected by AE species. By this, slabs of binary double layers (AE_5N_4) are formed which are part of distorted edge sharing octahedra NAE_5Co (blue/turquoise). In the crystal structure of $BaCa_4[CoN_2]_2$ Ba (*) takes the position which is in square planar coordination by N, whereas the coordination sphere of the other AE species (Ca) resembles a distorted tetrahedron.

Nitridocobaltates

$Ca_5[Co^IN_2]_2$ [7,8], **$Sr_5[Co^IN_2]_2$** [7], and **$BaCa_4[Co^IN_2]_2$** [7,12] are members of a novel series of isotypic nitridocobaltates $AE_5[Co^IN_2]_2$ (*P*4/*ncc* (No. 130)) containing linear $[Co^IN_2]^{5-}$ units; the crystal structures (Fig. 2) are isotypic to the nitridocuprate $BaCa_4[CuN_2]_2$ [13].

$Ca_5[CoN_2]_2$ nicely exemplifies the problems associated with the synthesis of nitridometalates: In 1993 the X-ray powder pattern and the lattice parameters of an alleged compound "$Ca_3Co^{III}N_3$" were reported [4], its composition being assigned in analogy to other $AE_3[MN_3]$ phases (e.g. $Ba_3[FeN_3]$ [14]) published at that time. However, the X-ray powder pattern of "$Ca_3Co^{III}N_3$" perfectly fits the pattern of $Ca_5[Co^IN_2]_2$ by assigning the additional reflections in the pattern to CaO [15] (Fig. 3).

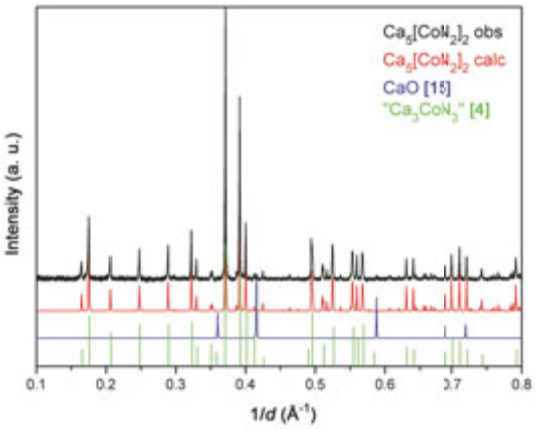

Fig. 3: Comparison of the X-ray powder patterns (from top to bottom) of $Ca_5[Co^IN_2]_2$ (observed), $Ca_5[Co^IN_2]_2$ (calculated), CaO, and "$Ca_3Co^{III}N_3$".

$Ba_9Ca[Co_2N_3]_3$ [7] represents the first example in nitridometalate crystal chemistry for the formation of ordered chain fragments $[M_2N_3]$.

The crystal structure of $Ba_9Ca[Co_2N_3]_3$ (trigonal, $P\bar{3}1m$ (No. 162), a = 9.7725(12) Å, c = 7.0063(11) Å, Z = 1) represents a novel structure type containing linear oligomers $[Co_2N_3]$. In addition to the rendering given in Fig. 4, the structure may be described as a defect perovskite ABO_3 = $A_9B_9O_{27}$ = $Ba_9(CaCo_6\square_2)(N_9\square_{18})$. According to established electron counting rules (Ba^{2+}, Ca^{2+}, N^{3-}), the oxidation number of Co is calculated to +1.17; the cause for this comparatively high value is still unclear. Chemical analyses present no indications of impurity effects. The investigation of the physical properties is currently underway.

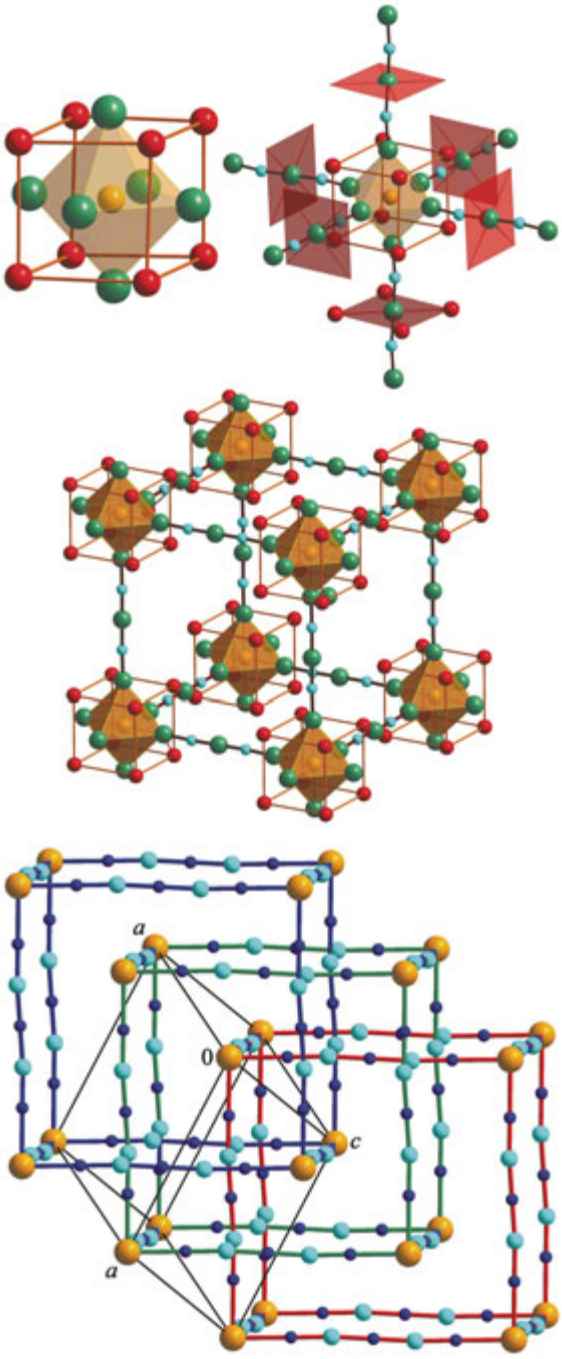

Fig. 4: The hierarchical construction of the crystal structure of $Ba_9Ca[Co_2N_3]_3$ (Ba: red, Ca: orange, Co: turquoise, N: green) is based on NCa_6 octahedra (top left) which are connected by $[Co_2N_3]$ units (top right) forming large cubes (center). The barium species (red spheres / red squares) complete the octahedral coordination of N, thereby forming a slightly distorted cubic primitive arrangement of Ba. The trigonal unit cell (black, bottom) generates three interpenetrating sets of equivalent cubes (red, green, blue).

Nitridometalate Carbodiimides

In the carbon containing systems, two different structure types of nitridometalate carbodiimides were identified under oxidizing (nitrogen-rich) conditions:

$Sr_6[M^{I}N_2]_2[CN_2]$ (M = Co [7,16], Ni [17]) crystallizes tetragonal in space group $I4/mmm$ (No. 139). The unique feature of the crystal structure (Fig. 5) is the mutual occupancy of the dumbbell positions with $[MN_2]^{5-}$ units (d(M–N) = 1.81 Å) and smaller $[CN_2]^{2-}$ units (d(C–N) = 1.23 Å).

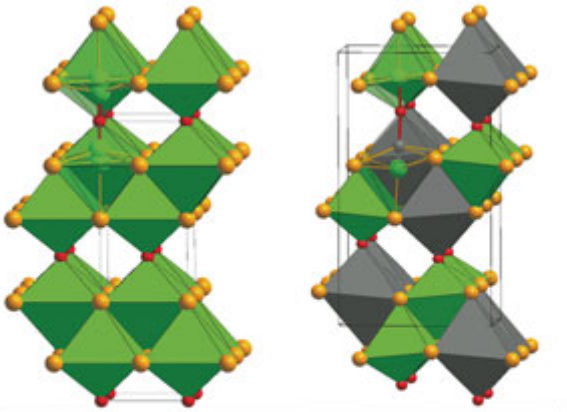

$Sr_6[M^{I}N_2]_2[CN_2]$	a [Å]	b [Å]	c [Å]
$Sr_6[Co^{I}N_2]_2[CN_2]$	3.8355(10)		12.378(4)
$Sr_6[Ni^{I}N_2]_2[CN_2]$	3.8223(2)		12.487(1)
$Sr_2[Ni^{0}(CN)N]$	7.815(5)	3.894(3)	13.998(19)

Fig. 5: Crystal structures of $Sr_6[M^{I}N_2]_2[CN_2]$ (left: (I), M = Co [7,16], Ni [17]) and $Sr_2[Ni^{0}(CN)N]$ [3,6] (right: (II). Both crystal structures are based on the $Na_2[HgO_2]$ structure type [18]; the doubling of the unit cell of $Sr_2[Ni^{0}(CN)N]$ (prepared under reducing conditions, space group Pnma (No. 62)) is due to the ordered distribution of the nitride and cyanide ions: $a_I \approx ½\ a_{II} \approx b_{II}$, $c_I \approx c_{II}$.

No ordering of the dumbbell species in the crystal structure of $Sr_6[M^{I}N_2]_2[CN_2]$ (M = Co, Ni) is evident; the refinement of the X-ray single crystal diffraction data clearly indicates a mixed occupancy $[MN_2]/[CN_2]$ (Fig. 6) in the approximate ratio 2:1, which would be consistent with established counting rules $Sr^{2+}{}_6[M^{I}N_2]^{5-}{}_2\ [CN_2]^{2-}$. The extent of a possible solid solution series $Sr_6[MN_2]_{2-x}[CN_2]_{1+x}$ is the topic of future research.

$(Sr_6N)[M^{I}N_2][CN_2]_2$ (M = Fe [7,19], Co [7,20], Ni [17]) crystallizes in space group $P2_12_12$ (No. 18) and contains nitridometalate dumbbells $[MN_2]^{5-}$, carbodiimide units $[CN_2]^{2-}$, and nitride ions N^{3-} in an ordered arrangement. The crystal

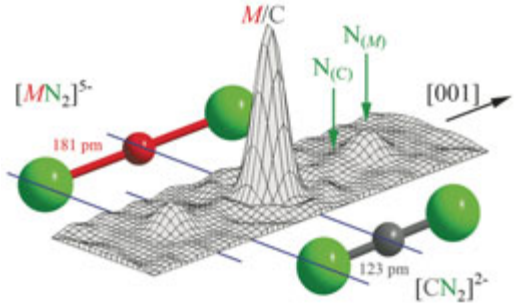

Fig. 6: Detail of the electron density distribution in the crystal structure of $Sr_6[M^{I}N_2]_2[CN_2]$. The assignment of the N species of the different dumbbells $[MN_2]^{5-}$ and $[CN_2]^{2-}$ is emphasized.

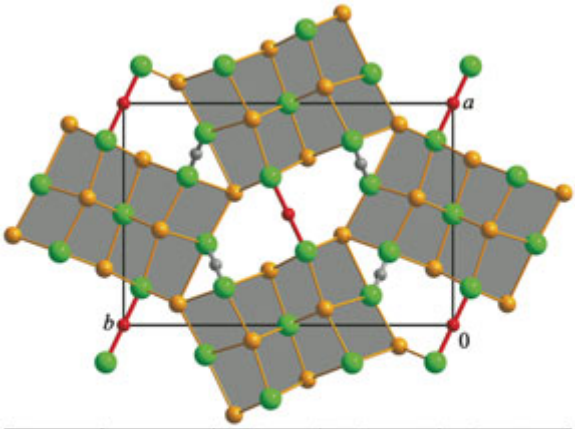

$(Sr_6N)[M^{I}N_2][CN_2]_2$	a [Å]	b [Å]	c [Å]
$(Sr_6N)[Fe^{I}N_2][CN_2]_2$	9.9367(6)	14.7275(9)	3.8553(3)
$(Sr_6N)[Co^{I}N_2][CN_2]_2$	9.8807(6)	14.6474(9)	3.8569(3)
$(Sr_6N)[Ni^{I}N_2][CN_2]_2$	9.8815(8)	14.6290(7)	3.8543(6)

Fig. 7: Crystal structure of $(Sr_6N)[M^{I}N_2][CN_2]_2$ (M = Fe [7,19], Co [7,20], Ni [17]). NaCl-like columns Sr_6N_7 (grey) are connected by $[CN_2]^{2-}$ and $[MN_2]^{5-}$ dumbbells.

structure (Fig. 7) can be described as an array of rocksalt-like columns Sr_6N_7 linked via common corners and connected by $[CN_2]^{2-}$ and $[MN_2]^{5-}$ units bridging the structural channels running along [001] within the rocksalt-like column arrangement.

On the Dimensionality of Complex Anions

The nitridometalates and nitridometalate carbodiimides presented in this report contain complex anions in the form of either dumbbells or short linear chain fragments (Fig. 8). M species are two-fold (linearly) coordinated by nitrogen. The coordination spheres around N are completed to (more or less distorted) octahedra by contacts to AE cations.

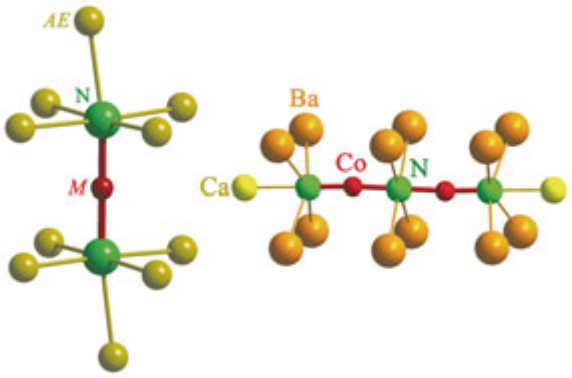

Fig. 8: Completed coordination spheres around a dumbbell $[MN_2]^{5-}$ (left: $AE_5[CoN_2]_2$, $Sr_6[MN_2]_2[CN_2]$, and $(Sr_6N)[MN_2][CN_2]_2$) and a chain fragment $[Co_2N_3]^{x-}$ (right: $Ba_9Ca[Co_2N_3]_3$).

The average bond lengths in the dumbbells $[MN_2]^{5-}$ (d(Co-N) = 1.82 Å and d(Ni-N) = 1.81 Å) and in the chain fragment $[Co_2N_3]^{x-}$ (d(Co-N) = 1.76 Å) are in the same range as observed in the already known compounds containing infinite nitridometalate chains and layers (d(Co-N) = 1.75 – 1.82 Å, d(Ni-N) = 1.77 – 1.82 Å).

Depending on the ratio *AE*:*M*, alkaline-earth nitridocobaltates and nitridonickelates contain complex anions of varying dimensionality (Tab. 1). As the coordination spheres of *M* (CN = 2) and N (CN = 6) hold for all the compounds under consideration, a preliminary rule may be stated: "The higher the ratio AE:M, the lower the dimensionality of the complex nitridometalate anion." This rule has to be checked during future work and by taking into consideration the existence of nitridometalate nitrides, such as $Ba_8[NiN]_6N$ [9].

Table 1: Dimensionality of complex anions in alkaline earth nitridocobaltates and -nickelates.

		ratio *AE*:*M*	complex anion
$Ba_2[Ni_3N_2]$	[3,10]	2:3 = 0.67	2D corrugated layer
Ca[NiN]	[21]	1:1 = 1	1D linear chain
Ba[CoN]	[22]	1:1 = 1	1D zig-zag chain I
Ba[NiN]	[23]	1:1 = 1	1D zig-zag chain II
$Ba_9Ca[Co_2N_3]_3$	[7]	10:6 = 1.67	0D oligomer $[Co_2N_3]$
$AE_5[CoN_2]_2$	[7,8,12]	5:2 = 2.5	0D dumbbell $[CoN_2]$

Physical Properties Investigations

Magnetic susceptibility measurements (Fig. 9) present information on the configuration of the *d* electron shell of the transition metals. For the isotypic compounds $AE_5[CoN_2]_2$ (AE_5 = Ca_5, $BaCa_4$) a

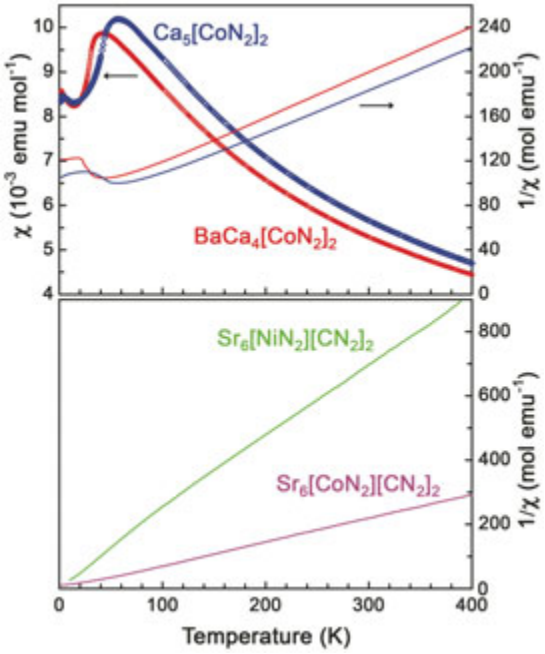

Fig. 9: Magnetic susceptibility data of selected nitridocobaltates and –nickelates. Symbols: χ(T) for a field of 1 T; lines: 1/χ(T) for a field of 7 T, corrected for ferromagnetic impurities.

paramagnetic effective moment corresponding to a state $S = 1$ and thus the d^8 configuration of Co^{I} can be assessed. Antiferromagnetic ordering transitions are visible at low temperatures. The same spin state of Co is observed in $Sr_6[CoN_2][CN_2]_2$ while the Ni isotype with $S = ½$ moments (d^9 configuration) corresponds to Ni^{I}.

Additionally, resistivity measurements have been performed to characterize some of the nitridocobaltate and nitridonickelate compounds: $Ca_5[CoN_2]_2$, $BaCa_4[CoN_2]_2$ and $Sr_2[Ni(CN)N]$ are insulators, $Ba_9Ca[Co_2N_3]_3$ is a semiconductor, and $(Sr_6N)[CoN_2][CN_2]_2$ shows metallic behavior.

X-ray absorption spectroscopy experiments (XAS, Fig. 10) were performed to obtain further information on the valence states of the transition metals. The XAS spectra of the nitridocobaltates show similar shapes, although the data for $Ba_9Ca[Co_2N_3]$ exhibit a small shift to higher energies and therefore rather support a structure model for Co with an oxidation state slightly different from +I as indicated in the charge balanced ionic formula $(Ba^{2+})_9(Ca^{2+})[(Co^{1.17+})_2(N^{3-})_3]_3$. XAS spectra of both strontium nitridonickelate-carbodiimides clearly show a similar behavior; compared to $Sr[NNi^{0}(CN)]$ and $Ba_2[Ni^{0,I}{}_2N_3]$ there is a small but significant shift to higher energies.

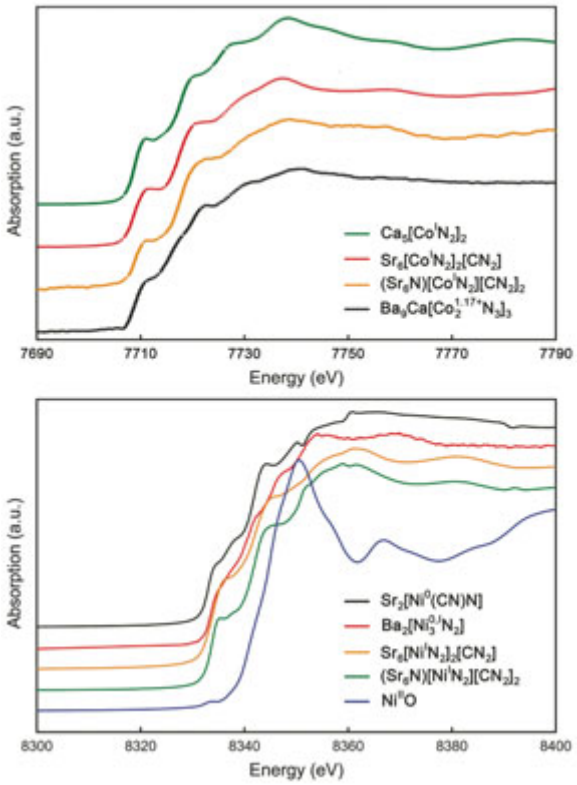

Fig. 10: XAS spectra of nitridocobaltates (top) and nitridonickelates (bottom) together with selected reference compounds.

Electronic Structure Calculations on $AE_5[Co^IN_2]_2$

In order to investigate the nature of the antiferromagnetic ordering in $BaCa_4[CoN_2]_2$ and $Ca_5[CoN_2]_2$ (Fig. 9), first-principles electronic structure calculations were performed using the full-potential all-electron code FPLO [24]. Both, the local spin density approximation (LSDA) and the LSDA+*U* scheme with the atomic-limit version of the double-counting correction were used to account for exchange and correlation effects.

No structural phase transitions were observed in the low-temperature X-ray diffraction investigations, which means that only ordering models without changes in the crystal structure had to be considered. Taking into account the group-subgroup relations (Fig. 11), all potential antiferromagnetic (AFM) ordering models for Co in the crystal structures of $Ca_5[CoN_2]_2$ and $BaCa_4[CoN_2]_2$ were identified and subsequently calculated.

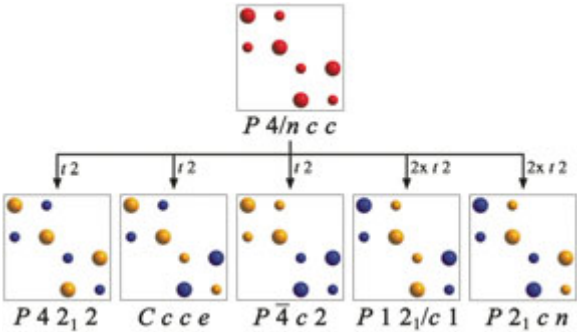

Fig. 11: Models for potential ordering of Co spins in the crystal structure of $AE_5[CoN_2]_2$ according to group-subgroup relations. Large spheres: z_{Co} = 0.25; small spheres: z_{Co} = 0.75; red: no ordering of spins; blue/yellow: ordering of spins. Only that part of the symmetry tree is shown which allows ordering in the corresponding highest symmetry for each ordering variant. The indicated subgroup unit cells do not necessarily coincide with the standard setting.

All LSDA calculations result in band gaps of about 0.4-0.5 eV, while the nonmagnetic calculation gives metallic DOS. Calculated band gaps increase to ~0.68 eV in LSDA+*U* calculations where *U* is taken as 6 eV. With regard to total energies, AFM arrangements are found to have lower total energies than ferromagnetic (FM) or nonmagnetic cases. The model with the lowest energy for $BaCa_4[CoN_2]_2$ is shown in Figure 12, and belongs to space group $P2_1cn$ (No. 33) as

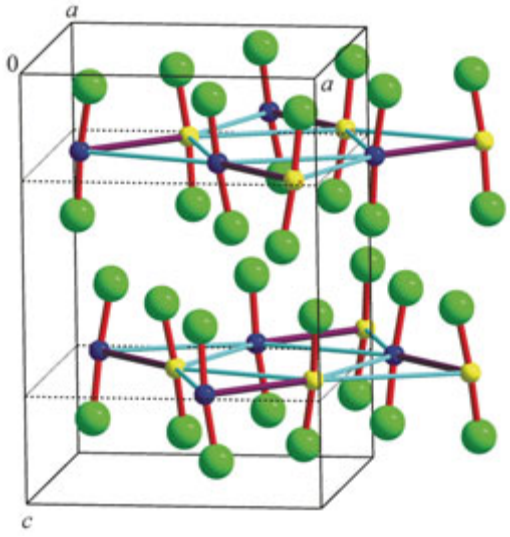

Fig. 12: AFM model with lowest energy for $BaCa_4[CoN_2]_2$. The two-dimensional projection of the unit cell in the Co layers is indicated by dotted black lines. Purple (turquoise) sticks denote the shortest (second shortest) Co-Co interactions. Blue and yellow circles represent Co atoms with up and down spins, respectively. N is represented by green circles, Ba and Ca are omitted for clarity.

depicted in figure 11. For $Ca_5[CoN_2]_2$ the lowest energy is obtained for the space group $P\bar{4}c2$ (No. 116). In the former (latter) model nearest neighbor Co atom pairs (Co dimers) are antiferromagnetically (ferromagnetically) coupled. The total energy differences between the AFM and FM configurations are mapped to a Heisenberg Hamiltonian. For $BaCa_4[CoN_2]_2$ we found that all exchange integrals up to the fifth neighbors had AFM signs with a strong interlayer Co-Co coupling. The nearest and next-nearest neighbor J values are comparable to the strongest interlayer coupling, all three having values on the order of 20 K. The third (intralayer) and fifth (interlayer) nearest neighbor couplings have values around 8 K.

Future Perspectives

The crystal chemistry of nitridonickelates and nitridocobaltates of alkaline earth metals and related nitridometalate carbodiimides has been extended towards alkaline-earth rich phases, which contain complex anions in the form of linear dumbbells $[M^{I}N_2]^{5-}$ or oligomers $[Co_2N_3]^{x-}$.

Future research will be focused on similar low-valency systems of the neighboring elements Mn, Fe, and Cu, respectively.

The authors gratefully acknowledge Dr. G. Auffermann, A. Völzke, and U. Schmidt for chemical analyses, R. Koban for electrical resistivity and magnetic susceptibility measurements, Dr. Yurii Prots for X-ray single crystal data collection and Steffen Hückmann for X-ray powder diffraction measurements. The authors also thank HASYLAB at DESY for supplying beamtime.

References

[1] *J. Klatyk, R. Niewa, F. R. Wagner, W. Schnelle, Z.-L. Huang, H. Borrmann, and R. Kniep*, in Scientific Report 2000, p. 116 (Max Planck Institute for Chemical Physics of Solids, Dresden Germany, 2000).

[2] *P. Höhn, R. Niewa, Z.-L. Huang, A. Mehta, V. Ivanshin, J. Sichelschmidt, Z. Hu, and R. Kniep*, in Scientific Report 2001/2002, p. 165 (Max Planck Institute for Chemical Physics of Solids, Dresden Germany, 2003).

[3] *P. Höhn, M. Armbrüster, G. Auffermann, U. Burkhardt, F. Haarmann, A. Mehta, and R. Kniep,* in Scientific Report 2003-2005, p. 206 (Max Planck Institute for Chemical Physics of Solids, Dresden Germany, 2006).

[4] *T. Yamamoto, S. Kikkawa, and F. Kanamaru*, Solid States Ionics **63-65** (1993) 148.

[5] *G. R. Kowach, N. E. Brese, U. M. Bolle, C. J. Warren, and F. J. DiSalvo*, J. Solid State Chem. **154** (2000) 542.

[6] *P. Höhn, M. Armbrüster, G. Auffermann, U. Burkhardt, F. Haarmann, A. Mehta, and R. Kniep*, Z. Anorg. Allg. Chem. **632** (2006) 2129.

[7] *J. K. Bendyna,* Dissertation, in preparation.

[8] *J. K. Bendyna, P. Höhn, and R. Kniep,* Z. Kristallogr. NCS **222** (2007) 165.

[9] *A. Gudat, W. Milius, S. Haag, R. Kniep, and A. Rabenau,* J. Less-Common Met. **168** (1991) 305.

[10] *A. Mehta, P. Höhn, W. Schnelle, V. Petzold, H. Rosner, U. Burkhardt, and R. Kniep*, Chem. Eur. J. **12** (2006) 1667.

[11] *E. Dashjav, G. Kreiner, W. Schnelle, F. R. Wagner, R. Kniep, and W. Jeitschko*, J. Solid State Chem. **180** (2007) 636.

[12] *J. K. Bendyna, P. Höhn, Yu. Prots, and R. Kniep,* Z. Kristallogr. NCS **222** (2007) 167.

[13] *R. Niewa and F. J. DiSalvo*, J. Alloys Comp. **279** (1998) 153.

[14] *P. Höhn, R. Kniep, and A. Rabenau,* Z. Kristallogr. **196** (1991) 153.

[15] *D. K. Smith and H. R. Leider*, J. Appl. Cryst. **1** (1968) 246.

[16] *J. K. Bendyna, P. Höhn, A. Ormeci, W. Schnelle, and R. Kniep,* J. Alloys Comp., in press.

[17] *P. Höhn, J. K. Bendyna, F. Nitsche, W. Schnelle, and R. Kniep,* Book of Abstracts, p. 296, SCTE 2008, 16th International Conference on Solid Compounds of Transition Elements, Dresden, Germany, 2008.

[18] *R. Hoppe and H. J. Roehrborn,* Naturwissenschaften **49** (1962) 419.

[19] *J. K. Bendyna, P. Höhn, and R. Kniep,* Z. Kristallogr. NCS, in press.

[20] *J. K. Bendyna, P. Höhn, W. Schnelle, and R. Kniep,* Science Tech. Adv. Mater. **8** (2007) 393.

[21] *A. Gudat, R. Kniep, and J. Maier,* J. Alloys Compd. **186** (1992) 339.

[22] *A. Tennstedt and R. Kniep,* Z. Anorg. Allg. Chem. **620** (1994) 1781.

[23] *A. Gudat, S. Haag, R. Kniep, and A. Rabenau,* J. Less-Common Met. **159** (1990) 29.

[24] *K. Koepernik and H. Eschrig,* Phys. Rev. B **59** (1999) 1743.